2018 IEEE Intelligent Vehicles Symposium (IV)
Changshu, Suzhou, China, June 26-30, 2018

Study on Vehicular Adaptive Cruise Control in Complicated Driving Conditions*

Xiujian Yang, Jinyu Li, Yifeng Cui

***Abstract*—This work concentrates on the problem of vehicular adaptive cruise control (ACC) in complicated driving conditions especially in low-adhesion road situations, and an ACC control scheme based on real-time estimation of road adhesion is proposed. The ACC controller is designed based on the model predictive control (MPC) method and the steady-state inter-vehicle spacing, relative velocity and the acceleration limits are incorporated into the MPC controller as the constraints. Thereby, the MPC problem is converted into the problem of optimal control with constraints and a receding-horizon approach is utilized to compute the desired vehicle acceleration. The real-time estimation of road adhesion coefficient is accomplished by the recursive least square (RLS) method. A four-degree-of-freedom (4DOF) nonlinear vehicle model is established based on the Lagrangian approach to act as the actual vehicle in the ACC system. The proposed ACC scheme is evaluated by simulations respectively in high and low adhesion conditions. The results reveal that collisions may occur in low adhesion condition if a fixed acceleration limit constraint is employed in the MPC control law. While the proposed adhesion-estimation based ACC system can accomplish the desired inter-vehicle distance safely.**

I. INTRODUCTION

The vehicle ACC system as an advanced driver assistance system (ADAS) is developed from the conventional cruise control system by adding the vehicle-following function. An ACC vehicle can detect the front road condition of a certain distance by radar, and then automatically adjusting the engine throttle, wheel driving/braking torque to control vehicle speed to improve the driving safety and comfortability. To keep reasonable inter-vehicle spacing under complicated conditions, a hierarchical control structure is often used in an ACC system. In detail, in the upper layer the desired vehicle acceleration is determined by the ACC controller and in the lower layer it is responsible for accomplishing the desired acceleration by appropriately adjusting the wheel driving/braking torque [1-3].

It is known that the MPC method is an effective means to solve the optimal control problem with multivariate constraints among the control algorithms of ACC systems, which consists of three essential elements: prediction model, receding-horizon optimization and feedback correction. The control action is obtained by resolving the optimal control of a finite time domain in each sampling period [4]. Consequently, the MPC method is believed to be effective to improve the control performance in terms of security and comfort for the ACC system. The existing ACC system generally takes driving safety as the main constraint [5], and in the design of ACC control law, it is commonly assumed that the driving state of the target vehicle varies abruptly. For instance, target vehicle moves slowly or completely stops; target vehicle brakes suddenly; target vehicle drives in a stop-and-go mode [5-10]. Under these complicated driving maneuvers, the ACC system of the following vehicle is designed to keep a safe inter-vehicle distance and avoids collision between the two vehicles.

Most of the current investigations about ACC system mainly focus on the cruise control algorithms which is usually tested and evaluated in high-adhesion road conditions. However, in actual applications, the road generally varies in a wide range of adhesion conditions. Particularly, in case of rather low-adhesion conditions, the ACC system may be not able to achieve the desired control objective, or even cannot avoid an inter-vehicle collision [11]. Therefore, in this work, a novel ACC control scheme is proposed which can automatically adjust the constraint of vehicle acceleration limit in the MPC controller by real-time estimation of road adhesion to adapt the complicated variation of road conditions. Here, the recursive least squares (RLS) method is employed for the road adhesion estimation and depending on which the MPC controller adjusts the acceleration limit to improve the ACC reliability and control performance.

II. NONLINEAR VEHICLE MODEL

In order to evaluate the proposed ACC control scheme from the viewpoint of practical application by simulation, in this section a 4DOF single-track nonlinear vehicle model based on the Lagrange's approach is developed to represent the actual vehicle. The four degrees of motion consists of the longitudinal motion, body pitch motion and rotational dynamics of the front and rear wheels. Fig. 1 illustrates the coordinate system and the schematic of body motion of this model.

The equations of motion are derived based on the Lagrange's approach which is a powerful modeling method for multi-body system. The nonlinear dynamical equation

This work is supported by Shandong Provincial Natural Science Foundation, China（Project No. ZR2015FL032）, A Project of Shandong Province Higher Educational Science and Technology Program（Project No. J13LN84）and NSFC (51465023).

Xiujian Yang is with the Kunming University of Science and Technology, Kunming, 650500 China, (Telephone: 13368806420; e-mail: yangxiujian2013@163.com).

Jinyu Li is with the Kunming University of Science and Technology, Kunming, 650500 China, (e-mail: 849625805@qq.com).

Yifeng Cui is with the Linyi University, Linyi, 276000 China, (e-mail: cuiyifeng@126.com)

depicting the longitudinal dynamics and the pitch motion respectively is given by Eq. (1) and Eq. (2) as following

$$\begin{aligned} &m\dot{v}_x + m\left(h_x \sin\theta + h_z \cos\theta\right)\ddot{\theta} + \\ &m\left(-h_z \sin\theta + h_x \cos\theta\right)\dot{\theta}^2 = F_{xf} + F_{xr} \end{aligned}, \tag{1}$$

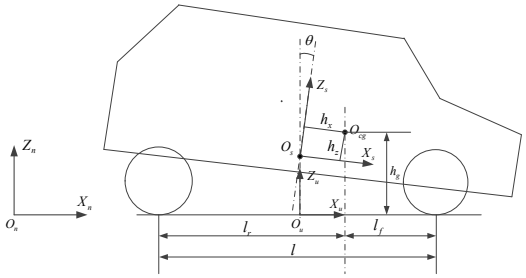

Figure 1 Vehicle coordinate system and the schematic of body motion

$$\begin{aligned} &m(h_z \cos\theta + h_x \sin\theta)\dot{v}_x + (mh_x^2 + mh_z^2 + I_y)\ddot{\theta} + mgh_x \\ &= F_{xf}(h_x \sin\theta - l_f \sin\theta) + F_{xr}(l_r \sin\theta + h_x \sin\theta) \\ &+ F_{zr}(l_r \cos\theta + h_x \cos\theta) + F_{zf}(h_x \cos\theta - l_f \cos\theta) \end{aligned}, \tag{2}$$

where θ denotes the pitch angle, h_x and h_z are used to identify the relative position between the pitch center O_s and the center of gravity O_{cg}, I_y denotes the moment of inertia of the pitch motion. The tire normal force for the front and rear wheel is respectively estimated as

$$F_{zf} = \frac{mgl_r}{l_f + l_r} - \frac{ma_x h_g}{l_f + l_r}, \tag{3}$$

$$F_{zr} = \frac{mgl_f}{l_f + l_r} + \frac{ma_x h_g}{l_f + l_r}, \tag{4}$$

where h_g is the height of the center of gravity. The longitudinal tire force F_{xf}, F_{xr} produced when braking or accelerating respectively for the front and rear wheel is calculated from pure longitudinal slip 'Magic Formula' tire model [12], which is formulated as

$$F_x = \mu D_x \sin\left(C_x \arctan\left(B_x \Phi_x\right)\right), \tag{5}$$

with

$$B_x = \frac{a_3 F_z^2 + a_4 F_z}{C_x D_x e^{a_5 F_z}},\ C_x = 1.65,$$

$$D_x = a_1 F_z^2 + a_2 F_z,\ E_x = a_6 F_z^2 + a_7 F_z + a_8,$$

$$\Phi_x = \left(1 - E_x\right)\sigma_x + \left(E_x / B_x\right)\arctan\left(B_x \sigma_x\right).$$

In tire model (5), μ denotes road adhesion coefficient, σ_x denotes longitudinal wheel slip and a_1~a_8 are empirical constant. The wheel slip is modeled as

$$\sigma_x = \frac{\omega_w r_w - v_x}{\omega_w r_w} \text{(Accelerating)}, \tag{6}$$

$$\sigma_x = \frac{\omega_w r_w - v_x}{v_x} \text{(Braking)}, \tag{7}$$

The wheel rotational angular velocity is determined by the wheel rotational dynamics equation

$$I_w \dot{\omega}_w = T_w - F_z f_r - F_x r_w, \tag{8}$$

where T_w is the braking/accelerating torque of the wheel and f_r is the rolling resistance coefficient. The effect of the power train system dynamics is described by a first order transfer function which will be presented in the following sections when designing the ACC control strategy.

As an illustration, here consider the following vehicle parameters m=1700kg, l_f=1.1m, l_r=1.6m, I_y=2700kg·m^2, h_z=0.045m, h_x=0.1m, h_g=0.3m, r_w=0.25m, I_w=12kg·m^2, f_r=0.02m, g=9.8. The response of the formulated 4DOF single-track nonlinear vehicle model to the wheel torque input given by Fig.2(a) is presented in Fig. 2 (b)~(d). It is noted that the response roughly agrees with the actual vehicle longitudinal dynamics behavior and the nonlinear tyre slip property.

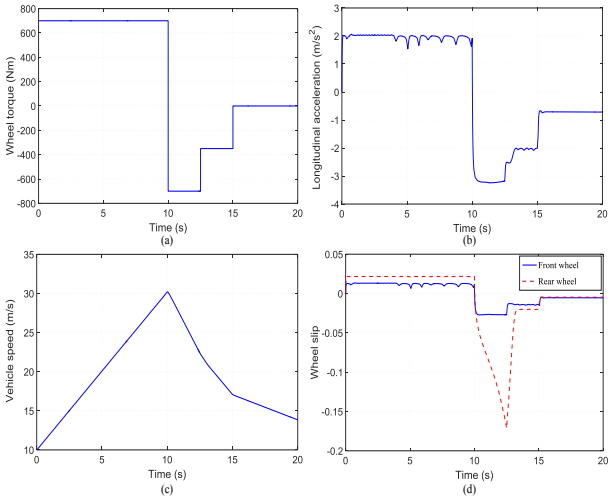

Figure 2. Illustration of the response of the 4DOF single-track nonlinear vehicle model.(a) Input wheel torque; (b) Response of longitudinal acceleration; (c) Response of vehicle speed; (d) Response of wheel slip.

III. Road Adhesion Estimation

From the point of vehicle dynamics, the vehicle acceleration limit is greatly dominated by the road adhesion condition. Thus, if the acceleration limit in the MPC-based ACC controller is set greater than the actual road adhesion, it is dangerous since it is easy to cause an inter-vehicle collision due to the insufficient braking capability. On the other hand, if the acceleration limit in the controller is set remarkably less than the actual road adhesion, the vehicle driving/braking capability cannot be used sufficiently. The nonlinear relationship between longitudinal friction coefficient and wheel longitudinal slip ratio is given by Fig. 3. In a small slip ratio range, the relation is approximately linear, which can be modeled as following [13]

$$\frac{F_x}{F_z} = k\sigma_x, \tag{9}$$

where k is the slope of longitudinal friction curve, F_x and F_z is the tire longitudinal and normal force respectively.

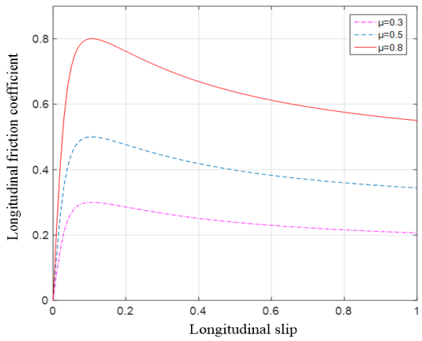

Figure 3. The nonlinear relationship between longitudinal friction coefficient and wheel longitudinal slip ratio.

First, express Eq.(9) to the form facilitating RLS estimation as following

$$y(t)=\varphi^{T}(t)\theta(t)+e(t), \tag{10}$$

with

$$y(t)=\frac{F_x}{F_z},\ \varphi(t)=\sigma_x,\ \theta(t)=k,$$

and $e(t)$ is the estimation error. The slope k is first estimated based on the RLS method, and then the tire-road friction coefficient can be obtained by [11]

$$\mu=k\times\sigma_m\times p, \tag{11}$$

where σ_m is the peak of longitudinal slip, p is the ratio of the maximum road adhesion in linear region to the peak road adhesion.

By introducing a forgetting factor λ in the RLS method to reduce the effect of old and useless information, an improved estimation method named RLS with the forgetting factor is obtained. Based on this improved estimation method, the road adhesion can be roughly estimated by the following steps[14].

Step 1: Take $\theta(0)=0$, $P(0)=10^{6}$, $\lambda=0.98$;

Step 2: Measure the output $y(t)$ and calculate the recursive matrix $\varphi(t)$;

Step 3: Calculate the estimation error

$e(t)=y(t)-\varphi^{T}(t)\theta(t-1)$;

Step 4: Calculate the gain matrix

$$K(t)=\frac{P(t-1)\varphi(t)}{\lambda+\varphi^{T}(t)P(t-1)\varphi(t)};$$

Step 5: Calculate the covariance matrix

$$P(t)=\frac{1}{\lambda}P(t-1)\left[I-K(t)\varphi^{T}(t)\right];$$

Step 6: Update $\theta(t)=\theta(t-1)+K(t)e(t)$.

The estimation of road adhesion based on RLS with forgetting factor is evaluated and illustrated in Fig.4 and Fig.5. As shown by the figures, the estimations of road adhesion are generally satisfying though there is a little difference in estimating precision in different case of road condition. However, in the authors' opinion, it is acceptable and it is important from the point of ACC system control application since this estimation can provide the MPC law with rough acceleration limit information. It is no doubt to be much helpful to improve the control performance of the MPC controller.

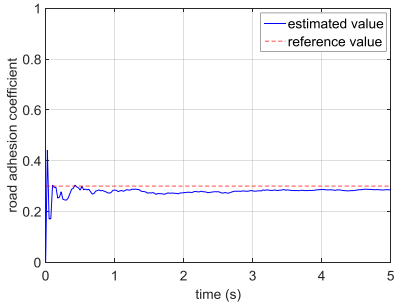

Figure 4. Road adhesion estimation for low adhesion condition (μ=0.3)

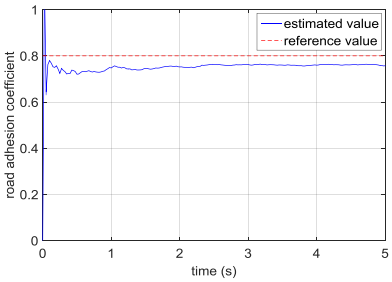

Figure 5. Road adhesion estimation for high adhesion condition (μ=0.8)

IV. MPC Based ACC Controller Design

The proposed ACC control scheme is of a two-layer structure which is illustrated in Fig.6.

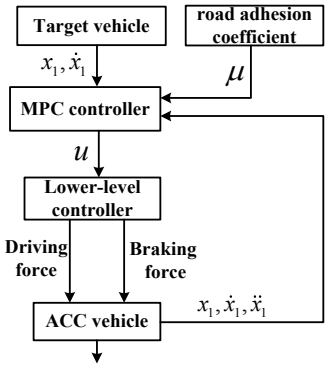

Figure 6.The overall structure of ACC system

As shown by the figure, the upper layer is a cruise controller based on the MPC control method with road adhesion estimation and this MPC problem will be further converted to the problem of optimal control with constraints which will be solved by the receding-horizon approach to compute the desired vehicle acceleration. The lower layer is responsible for accomplishing the desired vehicle acceleration commanded by the upper layer by regulating the wheel rotational dynamics. Especially in critical situations, e.g. hard braking/driving on slippery road, the lower layer needs to try to regulate the wheel slip to keep vehicle longitudinal dynamics stable.

A. The Discrete State Space Model of the ACC System

The schematic of a two-vehicle ACC system is shown in Fig.7. In the figure, x_1 and x_2 respectively represents the

position of the target vehicle and the ACC vehicle. The discrete state space model of the ACC vehicle is given as

$$\begin{pmatrix} x_2(t+T) \\ \dot{x}_2(t+T) \\ \ddot{x}_2(t+T) \end{pmatrix} = \begin{pmatrix} 1 & T & 0 \\ 0 & 1 & T \\ 0 & 0 & 1-\frac{T}{\tau} \end{pmatrix} \begin{pmatrix} x_2(t) \\ \dot{x}_2(t) \\ \ddot{x}_2(t) \end{pmatrix} + \begin{pmatrix} 0 \\ 0 \\ \frac{T}{\tau} \end{pmatrix} u(t), \tag{12}$$

where τ is a time constant representing the vehicle driveline dynamics and T is the discrete sampling time.

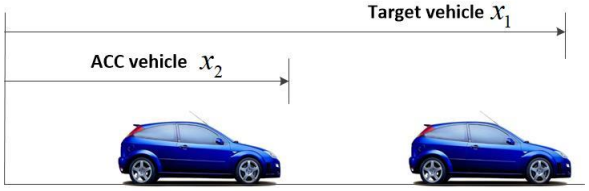

Figure 7.Two-vehicle ACC system

Here, the constant time-gap (CTG) spacing policy which is also called the constant time headway (CTH) policy in some literatures is adopted to keep a safe inter-vehicle distance. In this policy, the safe inter-vehicle distance varies linearly with the target vehicle speed, which is modeled as

$$S = h\dot{x}_1. \tag{13}$$

Fig.8 illustrates the motion of an ACC vehicle relative to the target vehicle in transitional maneuver state. The spacing error and the relative velocity between vehicles is the respectively expressed as $e_{12} = -(R-S)$, $\dot{e}_{12} = \dot{x}_2 - \dot{x}_1$.

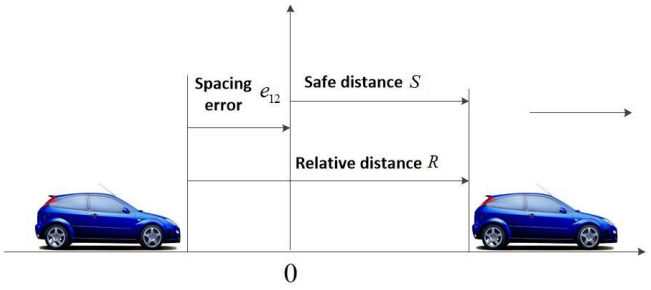

Figure 8. Coordinate of the two-vehicle ACC system in transitional maneuver state.

The discrete state space model of the two-vehicle ACC system can be expressed as

$$x(k+1) = Ax(k) + Bu(k), \tag{14}$$

$$y(k) = Cx(k), \tag{15}$$

with

$$A = \begin{pmatrix} 1 & T & 0 \\ 0 & 1 & T \\ 0 & 0 & 1-\frac{T}{\tau} \end{pmatrix}, \quad B = \begin{pmatrix} 0 \\ 0 \\ \frac{T}{\tau} \end{pmatrix},$$

$$C = \begin{pmatrix} 1 & 0 & 0 \\ 0 & -1 & 0 \end{pmatrix},$$

where $x(k) = \begin{bmatrix} e_{12} & \dot{e}_{12} & \ddot{x}_2 \end{bmatrix}^T$ is the system state, $u(k)$ and $y(k)$ is respectively the system input and output.

B. Objective Function and Constraints

The objective function is formulated as

$$J = \left\| x(N) \right\|_S^2 + \sum_{k=0}^{N-1} \left[\left\| x(k) \right\|_Q^2 + \left\| u(k) \right\|_R^2 \right], \tag{16}$$

where the weight matrix $Q = Q^T \geq 0$, $R = R^T > 0$, $S = S^T \geq 0$.

The solution of system state equation that is Eq. (14) can be expressed as:

$$x(k) = A^k x(0) + \sum_{l=0}^{k-1} A^l B u(k-1-l), \tag{17}$$

Rewrite Eq. (17) to a compact form as following

$$X = \bar{A}x(0) + \bar{B}U, \tag{18}$$

with

$$X = \begin{bmatrix} x(1) & \cdots & x(N) \end{bmatrix}^T, \bar{A} = \begin{bmatrix} A & \cdots & A^N \end{bmatrix}^T,$$

$$\bar{B} = \begin{bmatrix} B & 0 & \cdots & 0 \\ AB & B & \ddots & \vdots \\ \vdots & \vdots & \ddots & 0 \\ A^{N-1}B & A^{N-2}B & \cdots & B \end{bmatrix},$$

$$U = \begin{bmatrix} u(0) & \cdots & u(N-1) \end{bmatrix}^T.$$

Expanding Eq. (16) follows

$$J = x^T(0)Qx(0) + X^T\bar{Q}X + U^T\bar{R}U, \tag{19}$$

with

$$\bar{Q} = \begin{pmatrix} Q & 0 & 0 & 0 \\ 0 & \ddots & \ddots & \vdots \\ 0 & \ddots & Q & 0 \\ 0 & \cdots & 0 & S \end{pmatrix}, \bar{R} = \begin{pmatrix} R & 0 & 0 & 0 \\ 0 & \ddots & \ddots & \vdots \\ 0 & \ddots & R & 0 \\ 0 & \cdots & 0 & R \end{pmatrix}.$$

Then by substituting Eq. (18) into Eq. (19), we get

$$J = x^T(0)\left(Q + \bar{A}^T\bar{Q}\bar{A}\right)x(0) + U^T\left(\bar{R} + \bar{B}^T\bar{Q}\bar{B}\right)U + 2x^T(0)\bar{A}^T\bar{Q}\bar{B}U \tag{20}$$

Let

$$E = \bar{R} + \bar{B}^T\bar{Q}\bar{B}, \quad F = x^T(0)\bar{A}^T\bar{Q}\bar{B},$$

and then rewrite Eq. (20) as

$$J = x^T(0)\left(Q + \bar{A}^T\bar{Q}\bar{A}\right)x(0) + U^TEU + 2FU, \tag{21}$$

with the final state constraint

$$x(N) = \begin{bmatrix} 0 & 0 & 0 \end{bmatrix}^T, \tag{22}$$

system output and input constraints

$$y(k) = \begin{pmatrix} e_{12} \\ -\dot{e}_{12} \end{pmatrix} \leq \begin{pmatrix} S \\ \dot{x}_1 \end{pmatrix}, \tag{23}$$

$$u_{\min} \le u(k) \le u_{\max} . \tag{24}$$

C. Transform the optimal control problem to the Quadratic Programming problem

By the definition of constraint (23), the system output constraint is given as

$$y(k) = Cx(k) \le \begin{pmatrix} S \\ \dot{x}_1 \end{pmatrix} = W , \tag{25}$$

and as an alternative it can be further written to the following compact form

$$Y = \bar{C}X \le \bar{W} , \tag{26}$$

with

$$Y = \begin{bmatrix} y(1) & \cdots & y(N) \end{bmatrix}^T , \bar{W} = \begin{bmatrix} W & \cdots & W \end{bmatrix}^T ,$$

$$\bar{C} = \begin{bmatrix} C & 0 & \cdots & 0 \\ 0 & C & \ddots & \vdots \\ \vdots & \ddots & \ddots & 0 \\ 0 & \cdots & 0 & C \end{bmatrix} .$$

Substituting Eq. (18) into Eq.(26) , follows

$$\bar{C}\bar{B}U \le \bar{W} - \bar{C}\bar{A}x(0) . \tag{27}$$

Also, the input constraint (24) can be written to the compact form

$$U_{\min} \le U \le U_{\max} , \tag{28}$$

with

$$U_{\max} = \begin{pmatrix} u_{\max} \\ \vdots \\ u_{\max} \end{pmatrix} , U_{\min} = \begin{pmatrix} u_{\min} \\ \vdots \\ u_{\min} \end{pmatrix} .$$

Combining Eq. (27) and Eq. (28) we get

$$L_{IN}U \le M_{IN} , \tag{29}$$

with

$$L_{IN} = \begin{pmatrix} \bar{C}\bar{B} \\ I \\ -I \end{pmatrix} , M_{IN} = \begin{pmatrix} \bar{W} - \bar{C}\bar{A}x(0) \\ U_{\max} \\ -U_{\min} \end{pmatrix} .$$

By Eq. (18) and Eq. (22), we can also derive

$$\begin{bmatrix} A^{N-1}B & A^{N-2}B & \cdots & B \end{bmatrix} U = x(N) - A^N x(0) , \tag{30}$$

or rewrite as

$$L_{EQ}U = M_{EQ} , \tag{31}$$

with

$$L_{EQ} = \begin{bmatrix} A^{N-1}B & A^{N-2}B & \cdots & B \end{bmatrix} ,$$

$$M_{EQ} = x(N) - A^N x(0) .$$

Therefore, the objective function Eq. (21) can be formulated to the following quadratic program (QP)

$$J = U^T EU + 2FU , \tag{32}$$

subject to

$$L_{IN}U \le M_{IN} , L_{EQ}U = M_{EQ} .$$

V. Simulations

In this section, the proposed MPC based control scheme with road adhesion estimation for the ACC system is evaluated by simulations. The scenario is assumed that the target vehicle traveling at the speed of 14m/s is detected by the ACC vehicle 55m behind the target vehicle running at the speed of 28m/s. In such situation, the ACC vehicle switches from the speed control mode to the headway control mode to keep a safe inter-vehicle distance.

Here, we consider two road adhesion conditions with the adhesion coefficient of 0.8 and 0.3 corresponding to the high and low adhesion respectively. The estimated adhesion in the ACC system is respectively 0.75 and 0.28 which will be provided to the MPC control law. Simulation results of the ACC vehicle response in these three adhesion conditions are presented in Fig.9~Fig.12. In each adhesion condition, the ACC vehicle responses with and without adhesion estimation in MPC controller are evaluated.

As shown by the figures, the difference of ACC vehicle responses in high adhesion condition with and without adhesion estimation is not obvious. However, in relatively low adhesion conditions see Fig. 11 and Fig.12, the inter-vehicle collision would happen if there is no adhesion estimation. It is noted that road adhesion estimation for the ACC system is rather necessary on slippery road. In fact, in such low adhesion condition the wheel rotational dynamics is generally difficult to keep stable and particularly things becomes even worse in ACC control case where the ACC vehicle not only needs to keep its dynamics stable but needs to follow the target vehicle at a certain desired distance.

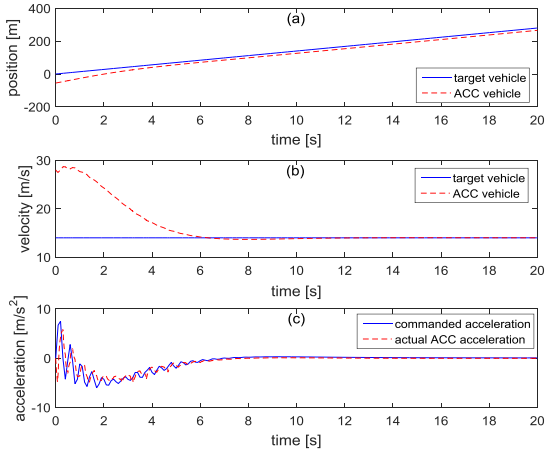

Figure 9 Responses of ACC vehicle in high adhesion condition (μ=0.8) with adhesion estimation

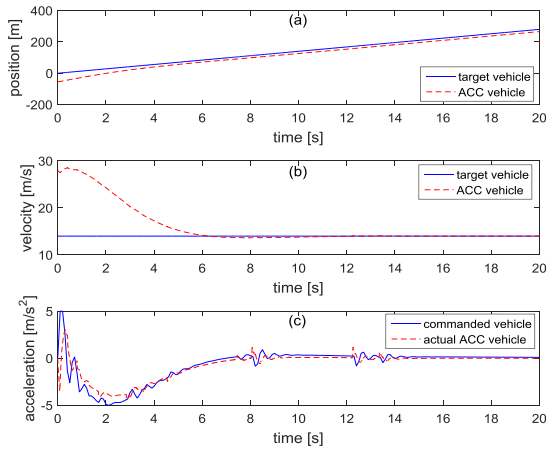

Figure10 Responses of ACC vehicle in high adhesion condition (μ=0.8) without adhesion estimation

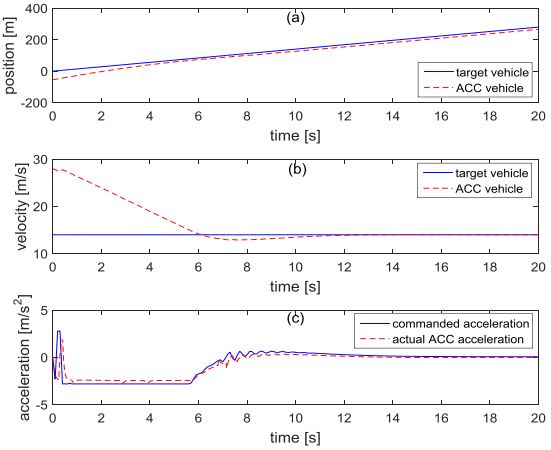

Figure11 Responses of ACC vehicle in low adhesion condition (μ=0.3) with adhesion estimation

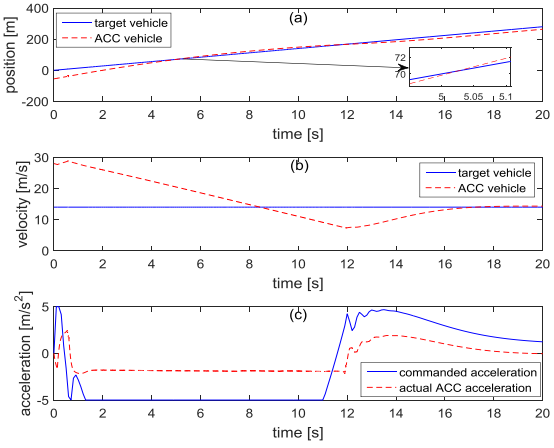

Figure12 Responses of ACC vehicle in low adhesion condition (μ=0.3) without adhesion estimation

VI. CONCLUSION

In this work, a novel ACC control scheme based on MPC control method is investigated. The main feature is that the vehicle acceleration limit in the MPC based ACC controller could be adjusted automatically depending on the real road condition by real-time adhesion estimation. The road adhesion estimator is designed based on the method of RLS with forgetting factor. The proposed ACC scheme is evaluated by simulations both in high and low adhesion conditions. As expected, it is revealed that collisions would happen in relatively low adhesion condition if a fixed acceleration limit constraint is set in the MPC based ACC controller. While the proposed control scheme with adhesion estimation can keep the desired following distance safely.

This work was supported by Shandong Provincial Natural Science Foundation, China（Project No. ZR2015FL032）, A Project of Shandong Province Higher Educational Science and Technology Program （Project No. J13LN84）and NSFC (51465023). The authors are greatly appreciated for the financial supports.

REFERENCES

[1] G. Wu, L. Zhang, Z. Liu, and X. Guo, “Research status and development trend of vehicle adaptive cruise control systems,” *Tongji Daxue Xuebao/Journal of Tongji University*, vol. 45, pp. 544-553, 2017. (In Chinese)

[2] E. Kural and B. A. Güvenç, “Model predictive adaptive cruise control,” in *IEEE International Conference on Systems Man and Cybernetics*, 2010, pp. 1455 - 1461.

[3] R. Attia, R. Orjuela, and M. Basset, “Combined longitudinal and lateral control for automated vehicle guidance,” *Vehicle System Dynamics*, vol. 52, pp. 261-279, 2014.

[4] L. Wang, “*Model predictive control system design and implementation using MATLAB®*,” Springer London, 2009.

[5] V. L. Bageshwar, W. L. Garrard, and R. Rajamani, “Model predictive control of transitional maneuvers for adaptive cruise control vehicles,” *Vehicular Technology IEEE Transactions on*, vol. 53, pp. 1573-1585, 2004.

[6] T. R. Connolly and J. K. Hedrick, “Longitudinal transition maneuvers in an automated highway system,” *Journal of Dynamic Systems Measurement & Control*, vol. 121, pp. 471-478, 1999.

[7] S. Li, K. Li, R. Rajamani, and J. Wang, “Model predictive multi-objective vehicular adaptive cruise control,” *IEEE Transactions on Control Systems Technology*, vol. 19, pp. 556-566, 2011.

[8] S. Li, K. Li, R. Rajamani, and J. Wang, “Multi-objective coordinated control for advanced adaptive cruise control system,” in *Decision and Control, 2009 Held Jointly with the 2009 Chinese Control Conference. CDC/CCC 2009. Proceedings of the IEEE Conference on, 2009*, pp. 3539-3544.

[9] J. J. Martinez and C. Canudas-De-Wit, “A safe longitudinal control for adaptive cruise control and stop-and-go scenarios,” *IEEE Transactions on Control Systems Technology*, vol. 15, pp. 246-258, 2007.

[10] van den Bleek, R. A. P. M. “Design of a hybrid adaptive cruise control stop-&-go system.” Master's Thesis, INO Science & Industry, Technische Universiteit Eindhoven (2007).

[11] B. Zhu, Q. Piao, J. Zhao, J. Wu, and W. Deng, “Vehicle longitudinal collision warning strategy based on road adhesive coefficient estimation,” *Qiche Gongcheng/automotive Engineering*, vol. 38, pp. 446-452, 2016. (In Chinese)

[12] E. Bakker, “A new tire model with an application in vehicle dynamics studies,” *SAE Technical Paper*, vol. 98, 1989.

[13] L. Alexander and R. Rajamani, “Friction estimation on highway vehicles using longitudinal measurements,” *Journal of Dynamic Systems Measurement & Control*, vol. 126, pp. págs. 265-275, 2004.

[14] L. I. Xuan-Zheng, “Tire-road friction coefficients estimation base on slip rate,” *Science & Technology Vision*, 2014. (In Chinese)